

Optimal Design of Wideband Array Patterns

Dan P. Scholnik and Jeffrey O. Coleman
Naval Research Laboratory
Washington, DC

Abstract— In radar systems, wideband array patterns are typically nothing but patterns designed in the conventional narrowband way and then time-delay steered. It is increasingly common to use digital filters to approximate the needed delays. We suggest, however, that approximating time delays is an inefficient use of the valuable resource represented by these filters and propose instead that their responses be jointly optimized to meet specifications on the array pattern as a function of angle and frequency. This frees the angle-dependence and frequency-dependence of the array function from the fixed relationship implied by time-delay steering and allows tremendous design flexibility, and it improves the tradeoff between filter length and ultimate array performance.

I. INTRODUCTION

Once computationally impractical, wideband digital antenna arrays are now a reality thanks to the continued evolution of computing power. Whereas formerly wideband arrays required switched analog delay elements and attenuators, now the (nonadaptive) array-pattern synthesis can be performed by digital filtering of data sampled at the antenna, with the usual gains in precision and flexibility. A conventional approach to digital pattern synthesis is to simply approximate the analog hardware with digital filters. This has the same drawback as the analog system it replaces—it places artificial restrictions on the resulting array pattern. In most cases even ideal time-delay steering results in a suboptimal array response. It seems appropriate to rethink the problem of array pattern design from first principles taking an optimization viewpoint, since the tools now exist [1–5] to solve large problems posed as convex programs.

We first present a quick review of the far-field equations for narrowband and wideband antenna arrays, along with the classic time-delay approach to wideband pattern synthesis. We then show through a progression of examples how direct optimization of the array response pattern itself with respect to frequency and angle offers greater flexibility and performance than the time-delay approach.

II. ARRAY BASICS

For clarity in the paper we will restrict our attention to a linear array of isotropic antenna elements placed along the x -axis. An extension to two and three dimensions is given in [6]. The angle θ is measured with respect to the x -axis, with zero degrees lying perpendicular to the axis. The constant c represents the velocity of radiation in free space.

A. Narrowband Array Pattern Response

The narrowband equation for the far-field pattern of a linear array of isotropic elements located at positions $\{x_k\}$ is usually

This work was supported by the Office of Naval Research through its program in Operations Research and through its Base Program at the Naval Research Laboratory.

given as

$$A(\theta) = \sum_k a_k e^{-j2\pi \frac{x_k}{\lambda} \sin(\theta)} \quad (1)$$

where λ is the radiating wavelength. The complex coefficients $\{a_k\}$ are chosen to steer the beam in the desired direction and to control sidelobes. This equation has the form of a Fourier transform to the variable $\sin(\theta)$, often denoted as u . When $x_k = kd$, then (1) can be written

$$A(u) = \sum_k a_k e^{-j2\pi k \left(\frac{d}{\lambda}\right) u}, \quad (2)$$

which is a discrete-time Fourier transform from index k to normalized frequency $\nu = ud/\lambda$. In the common case where $d = \lambda/2$, $\theta \in [-90^\circ, 90^\circ]$ corresponds to $\nu \in [-0.5, 0.5]$, and the semicircle of physical angles maps exactly to one period of the Fourier transform response. If $d < \lambda/2$ the semicircle maps to less than a full period, and thus there exists a range of values of ν that do not correspond to any physical angle, and the transform response in that region (the nonvisible sidelobes) does not directly affect the array pattern (more on this later). If $d > \lambda/2$ the semicircle maps to greater than one period of the transform response. This is usually undesirable, since any part of the array pattern corresponding to a single period of the Fourier transform completely determines the rest of the pattern, leading to grating lobes at high angles.

In all three cases the design of the coefficients $\{a_k\}$ is directly analogous to the design of an FIR filter over an appropriate range of frequencies. FIR filter design is a mature subject, and the design technique of interest here is convex programming. Convex-optimization-based approaches to the design of narrowband array patterns and FIR responses can be found in [1, 2, 6–13].

B. Extending To Wideband

The above analysis is valid for a single wavelength λ , but in the wideband case λ will cover a range of wavelengths. Thus we wish to consider the array pattern as a function of radiating frequency as well as angle. Substituting $\lambda = c/f$ in (1) results in

$$A(u, f) = \sum_k a_k e^{-j2\pi \frac{f x_k}{c} u},$$

and increasing or decreasing the radiating frequency has the effect of scaling the beam in angle. When the beam is not pointed to zero angle (boresight), this results in the beam

changing both in width and direction with frequency, an effect known informally as beam squint. The solution to this problem is to replace complex weight a_k with frequency response $H_k(f)$, so that the effective array weighting can vary over the bandwidth of interest. This specializes to the conventional time-delay array architecture in which

$$H_k(f) = b_k e^{j2\pi \frac{f x_k}{c} u_0},$$

with $\{b_k\}$ a set of real weights and $u_0 = \sin(\theta_0)$ the desired pointing direction. This choice for $H_k(f)$ corrects for the delay of a plane wave arriving from angle θ_0 as seen by element k (relative to the origin). The resulting array response is

$$A(u, f) = \sum_k b_k e^{-j2\pi \frac{f x_k}{c} (u - u_0)}, \quad (3)$$

which at any frequency f is just the response of the narrowband boresight beam defined by the coefficients $\{b_k\}$ but scaled by f and shifted in u to the desired angle. Thus the beam direction problem is alleviated, but the scaling by f results in an array pattern that compresses (becomes narrower) as the frequency increases. The ratio of the maximum to the minimum size (measured in u) of a given feature is proportional to the ratio of high to low radiating frequency.

C. DSP Realization

We consider here primarily receive arrays (although analysis of transmit arrays is essentially identical) since the transmit power requirements of modern radar systems usually limits the transmit beamforming choice to straight time delay with a uniform weighting across the elements. There are several functionally equivalent ways to implement a wideband digital receive array, but for our purposes we consider a simplified model in which the bandpass signal at each antenna element is sampled and converted to an analytic (spectrally one-sided) bandpass digital signal prior to digital beam combining at the RF frequency. In practice the downconversion step may occur before or after beamforming, which primarily affects whether the beamforming filters have real coefficients and operate at the initial sampling rate (before downconversion) or have complex coefficients and operate at a lower sampling rate (after downconversion).

If we consider the array pattern formed using FIR filters at each element, the result is

$$\begin{aligned} A(u, f) &= \sum_k H_k(f) e^{-j2\pi \frac{f x_k}{c} u} \\ &= \sum_k \sum_n h_{k,n} e^{-j2\pi n f T} e^{-j2\pi \frac{f x_k}{c} u} \end{aligned} \quad (4)$$

At all frequencies and angles $A(u, f)$ is linear in the filter coefficients $\{h_{k,n}\}$, which conveniently permits a great number of common constraints to be expressed in terms of convex functions of the coefficients as the optimization variables. This in turn allows design of the array pattern using convex optimization tools[1, 2, 7]. In the common symmetric-array case, for which $x_{-k} = -x_k$, the additional requirement that

$H_{-k}(f) = H_k^*(f)$, or its equivalent $h_{-k,-n} = h_{k,n}^*$, ensures that $A(u, f)$ is real-valued (a linear-phase response). This not only reduces by one half the number of variables to optimize, but can be exploited to reduce real-time computation requirements as well. Unless a specific (nonlinear) phase response is desired, these significant benefits come with no ill effects.

III. DESIGN APPROACH

In this section, we demonstrate the flexibility of a convex-optimization approach to array pattern design through a series of examples. The goal here is not the realization of an actual design so much as it is to develop insight into the design issues associated with directly optimizing the wideband array pattern. We first discuss an example design in which the beam is steered with ideal time delays and then a second in which those delays are approximated with individually optimized FIR filters. Then we present two designs in which the FIR coefficients are jointly optimized to directly tailor the array function. In the first of these, the main-beam characteristics of the ideal time-delay design are essentially duplicated but with a performance gain in the sidelobes resulting from the joint optimization. The final example, which represents our recommended approach, illustrates the idea of really tailoring the constraints to the application to take advantage of the flexible control over the pattern afforded by the optimization approach.

The system parameters are the same for all cases except the first, which uses ideal time delays instead of FIR filters. The RF center frequency is at 1.25 GHz, the system bandwidth is 400 MHz, and the data is sampled at a rate of 1 GHz. The array is composed of 15 identical isotropic elements, each feeding a 21-tap, real-coefficient, nonlinear-phase FIR filter. The filters obey the symmetry discussed above, so that $H_0(f)$ is itself linear-phase and $H_{-k}(f) = H_k^*(f)$ for $k = 1, \dots, 7$. The spacing between the elements is set to one half wavelength at the highest in-band frequency of 1.45 GHz in order to suppress grating lobes at lower frequencies. In each case a pattern is designed with a center at 45° and a maximum sidelobe height of -25 dB.

A. Ideal Time Delay

As seen previously, when ideal time delays are used, wideband pattern synthesis reduces to the narrowband case, with each element's delayed waveform receiving a single real weight. The result is a wideband pattern which at each frequency has an angular response of the form of the narrowband pattern, scaled by the frequency. In classic narrowband pattern synthesis, two classic approaches stand out. The first is Chebychev beam design, which seeks the narrowest beamwidth for a given sidelobe level, or alternatively the lowest sidelobe level for a given beamwidth. In practice a Chebychev design is usually easily improved upon, since a small increase in the close-in sidelobes can often lead to large reductions in the outer sidelobes [7]. Taylor [14] proposed a now-classic alternative: require (nearly) equiripple sidelobes close to the mainlobe, with monotonic falloff of sidelobe peaks outside of some interval. The resulting continuous Taylor distri-

bution and its sampled version are often used in arrays.

In the spirit of Taylor's approach, but to facilitate comparison with later examples, we can design a narrowband beam according¹ to:

$$\begin{aligned} & \text{minimize} && \int_{\theta \in \Theta_{\text{sb}}} |A(\theta)|^2 d\theta \\ & \text{subject to} && |A(\theta)| \leq 10^{-25/20}, \quad \theta \in \Theta_{\text{sb}} \\ & && A(0) = 1 \end{aligned}$$

where Θ_{sb} denotes the stopband or sidelobe region. Since the coefficients are real, $A(\theta)$ and Θ_{sb} are symmetric about zero degrees. The boresight pattern thus optimized has the lowest sidelobe energy for the given maximum sidelobe level and beamwidth, however this is no longer true once the pattern has been shifted by u_0 as in (3). These weights can then be used along with ideal time delays to form a wideband array pattern, as illustrated in the top half of fig. 1, which shows the resulting pattern as a two-dimensional function of θ and f in addition to one-dimensional slices along both dimensions.

Two features of this response are especially notable. The first is that the beam does in fact narrow with increasing frequency, a consequence of the scaling by f in the wideband equation. Moreover, the compression effect and the main beam itself are not symmetric about the center of the beam—the higher angles compress more rapidly. This is because the quantity scaled by f is $u = \sin(\theta)$, and not θ itself, and at higher angles θ is a more sensitive function of u . The second notable feature is that the frequency response at off-center angles rolls off at higher frequencies, a direct consequence of the beam-narrowing effect. This rolloff becomes more pronounced at angles further from the center of the beam. In some applications this rolloff may be unacceptable, and so in a later example (the last one) we will consider ways to remove it.

The primary advantage of time-delay beamforming is that it only requires the design of a single narrowband weighting function, which is used for all steering directions. The disadvantages are the high-frequency response rolloff and the sub-optimality of the antenna pattern, as well as the difficulty in obtaining high-precision, high-resolution delay elements.

B. FIR Time Delay Approximation

Digital beamsteering architectures replace traditional switched analog delay lines with digital filters to approximate arbitrary time delays. One can either use a library of filter weights corresponding to the needed set of closely spaced delays, or one can use a single filter tunable in delay [15]. The optimization is more easily discussed assuming the fixed delays of a library, and so that is the approach taken here, but similar strategies could also be used to improve a tunable delay filter.

A straightforward design approach² for a minimum mean square error FIR filter approximating delay τ is

¹Refs. [1, 2, 7, 11] discuss how to formulate these and other type of constraints for numerical solution.

²So straightforward, in fact, that convex optimization is not required unless auxiliary constraints are desired.

$$\text{minimize} \quad \int_{f \in \mathcal{F}_{\text{pb}}} |H(f) - e^{-j2\pi f\tau}|^2 df,$$

where \mathcal{F}_{pb} is the passband region. The bottom half of fig. 1 shows the array pattern that results from using a set of delay filters so designed. Amplitude ripple has been introduced into the frequency response in the main beam, and some fine sidelobe structure differs, but otherwise the pattern resembles that of the ideal case. The approximation errors in the delay filters determine both the size of the amplitude ripples in the main beam and the fidelity with which the pattern's sidelobe structure duplicates that of the ideal frequency-scaled narrowband pattern. With this architecture then, the main-beam and sidelobe error structures cannot be independently controlled or traded off against each other. The overall pattern is also sub-optimal since the delays are designed independently and not jointly.

C. Direct Beam Optimization

While it is true that having each filter approximate a delay results in a useful pattern in angle-frequency space, there are many other filter combinations that would presumably do so as well, and since there is no reason to presume that the time-delay approach results in the best one, it amounts to an inherent structural restriction in the design that holds that design away from optimality. Here we consider the much more flexible approach of directly constraining the wideband array pattern. By only enforcing constraints that are meaningful for a given application and avoiding inherent structural restrictions, we obtain better designs.

The following optimization setup was used for the last two examples:

$$\begin{aligned} & \text{min.} && \int_{f \in \mathcal{F}_{\text{pb}}} \int_{\theta \in \Theta_{\text{sb}}(f)} |A(\theta, f)|^2 d\theta df \\ & \text{s.t.} && |A(\theta, f)| \leq 10^{-25/20}, \quad \theta \in \Theta_{\text{sb}}(f), \quad f \in \mathcal{F}_{\text{pb}} \\ & && \int_{f \in \mathcal{F}_{\text{pb}}} |A(\theta_m, f) - \beta_m|^2 df \leq \delta, \quad m = 1, \dots, M \\ & && \frac{1}{M} \sum_m \beta_m = 1 \\ & && \sum_k \|h_k\|^2 \leq \epsilon \end{aligned}$$

Here we seek to minimize the total energy in the in-band sidelobe region defined by \mathcal{F}_{pb} and Θ_{sb} (which may be a function of frequency), subject to several constraints. The first sets a maximum sidelobe level of -25 dB for all in-band frequencies and for angles in Θ_{sb} . The second and third constraints control the mainlobe frequency response in the passband. The second constraint introduces auxiliary variables $\{\beta_m\}$, which represent desired gain levels of the array pattern at angles $\{\theta_m\}$ in the main beam. The square passband error at each angle θ_m is limited to some constant δ . By using auxiliary variables, the desired gain at each angle is allowed to float rather than being fixed. The third constraint then fixes the average gain of the main beam, which is needed to prevent the optimization from

returning all zeros.

The last constraint limits the white-noise gain of the set of filters to a constant ϵ . Why might this constraint be needed? Recall from before that when $d < \lambda/2$ for a narrowband array, part of the DTFT of the array coefficients does not map to any physical angles. Since d here is half of the smallest wavelength of interest, this condition will hold for all frequencies in the band of interest except for the upper band edge. None of the other constraints directly limits the response in this nonvisible region, and left unconstrained it can grow quite large. While it has no direct effect on the antenna pattern (which measures the response to incident plane waves), the entire DTFT does respond to independent white receiver noise, and the result is an excessive noise gain and filter coefficients with a higher dynamic range. Choosing a modest limit on the total noise gain solves the problem, while still allowing the optimization to adjust the nonvisible portion of the response as needed to optimize the visible portion. This is an advantage over time-delay designs, which suppress the nonvisible sidelobes as much as the visible ones.

As a bridge from the FIR time-delay design example, we first consider a design in which the sidelobe region is chosen to match that of the time-delay case so that Θ_{sb} consists of the interval $[-90^\circ, 90^\circ]$ minus an asymmetric interval about 45° that narrows with increasing frequency. Optimizing as shown above with a single constraint limiting the rms frequency response error at 45° to 1% results in the response in the top plot of Fig. 2. The main beam is essentially identical to that of the time-delay design, as is the frequency response at the beam's center. The overall sidelobe level is lower, especially at lower frequencies, and the sidelobe structure is no longer forced to be unchanging across frequency. This is a result of designing the filters jointly and not separately as in the time-delay design and of removing the implicit structural restriction on the mainbeam shape. The design cost is now significantly higher, as a complete set of filter coefficients must be computed for each look direction, but the implementation cost is as before.

While better than the time-delay design, the design just described has obvious drawbacks. The frequency response at off-center angles in the main beam could be improved, and the beam still changes width with frequency. For the final design example, then, the sidelobe region is chosen to be constant (not a function of frequency) with a beamwidth slightly narrower than the maximum beamwidth of the previous designs, and the rms frequency response error is constrained to 0.1% for $\theta \in [42^\circ, 48^\circ]$. The noise gain was limited to the same level as in the previous design. To demonstrate the ability to custom tailor the sidelobe distribution in both frequency and angle an additional constraint was used, limiting the response on the region between -10° and 10° in angle and 1.1 GHz and 1.2 GHz in frequency to less than -45 dB. The optimized response is shown in the bottom plot of Fig. 2. Note that the beamwidth is in fact nearly constant and that the frequency response in the main beam is much better than that of previous designs. Even though the improved passband and custom sidelobe constraints necessarily increase the sidelobe energy, it is roughly the same as for the previous design and better

than for the time-delay examples. Removing the frequency-dependent constraint on the sidelobe region and directly optimizing the wideband array pattern has resulted in a substantial performance gain over the conventional time-delay method.

IV. CONCLUSIONS

The design examples presented only scratch the surface of the possibilities that convex optimization has to offer in wideband array pattern design. The key is the flexibility it affords to custom tailor sidelobe structure and main-beam shape to detailed system requirements. In the spirit of the angle- and frequency-limited region of extra suppression in the final design, a design can accommodate known features such as fixed clutter (a notch in angle) or sources of narrowband interference (a notch in both angle and frequency). In principle this approach can be generalized to multidimensional arrays of arbitrary geometry, including sparse arrays and arrays with random element placement. Work remains, however, in devising efficient optimization formulations to make this approach practical for arrays exceeding a few hundred elements.

REFERENCES

- [1] L. Vandenberghe and S. Boyd, "Semidefinite programming," *SIAM Review*, vol. 38, no. 1, pp. 49–95, Mar. 1996.
- [2] M. S. Lobo, L. Vandenberghe, S. Boyd, and H. Lebret, "Applications of second-order cone programming," *Linear Algebra and its Applications*, vol. 284, pp. 193–228, Nov. 1998.
- [3] R. Vanderbei, "LOQO: An interior point code for quadratic programming," Technical Report SOR 94-15, Princeton University, 1994, revised 11/30/98, to appear in *Optimization Methods and Software*.
- [4] J. F. Sturm, "Sedumi," MATLAB toolbox, May 1998, <http://www.unimaas.nl/~sturm/software/sedumi.html>.
- [5] S. Boyd, L. Vandenberghe, and M. Grant, "Efficient convex optimization for engineering design," in *Proc. IFAC Symposium on Robust Control Design*, Rio de Janeiro, Brazil, Sept. 1994.
- [6] J. O. Coleman and R. J. Vanderbei, "Random-process formulation of computationally efficient performance measures for wideband arrays in the far field," in *Proc. Midwest Symp. on Circuits and Systems (MWSCAS)*, Las Cruces, NM, Aug. 1999.
- [7] J. O. Coleman and D. P. Scholnik, "Design of nonlinear-phase FIR filters with second-order cone programming," in *Proc. Midwest Symp. on Circuits and Systems (MWSCAS)*, Las Cruces, NM, Aug. 1999.
- [8] D. P. Scholnik and J. O. Coleman, "Nonuniformly offset polyphase synthesis of a bandpass signal from complex-envelope samples," in *Proc. 1999 Int'l Symp. Circuits and Systems (ISCAS '99)*, Orlando, FL, May 1999.
- [9] W.-S. Lu, "Design of nonlinear-phase FIR digital filters: A semidefinite programming approach," in *Proc. 1999 Int'l Symp. Circuits and Systems (ISCAS '99)*, Orlando, FL, May 1999.
- [10] H. Lebret and S. Boyd, "Antenna array pattern synthesis via convex optimization," *IEEE Trans. on Signal Processing*, vol. 45, no. 3, pp. 526–32, Mar. 1997.
- [11] J. O. Coleman, "Systematic mapping of quadratic constraints on embedded FIR filters to linear matrix inequalities," in *Proc. 1998 Conference on Information Sciences and Systems (CISS '98)*, Princeton, NJ, Mar. 1998.
- [12] K. Steiglitz, T. W. Parks, and J. F. Kaiser, "METEOR: A constraint-based FIR filter design program," *IEEE Trans. Signal Processing*, vol. 40, no. 8, pp. 1901–1909, Aug. 1992.
- [13] J. O. Coleman, "Linear-programming design of hybrid analog/FIR receive filters to minimize worst-case adjacent-channel interference," in *Proc. Conf. on Information Sciences and Systems*, Baltimore, MD, Mar. 1993.
- [14] T. T. Taylor, "Design of line-source antennas for narrow beamwidth and low sidelobes," *IRE Trans. Antennas Propag.*, vol. AP-3, no. 1, pp. 16–28, Jan. 1955.
- [15] W.-S. Lu and T.-B. Deng, "An improved weighted least-squares design of FIR digital filters with variable fractional delay," in *Proc. 1999 Int'l Symp. Circuits and Systems (ISCAS '99)*, Orlando, FL, May 1999.

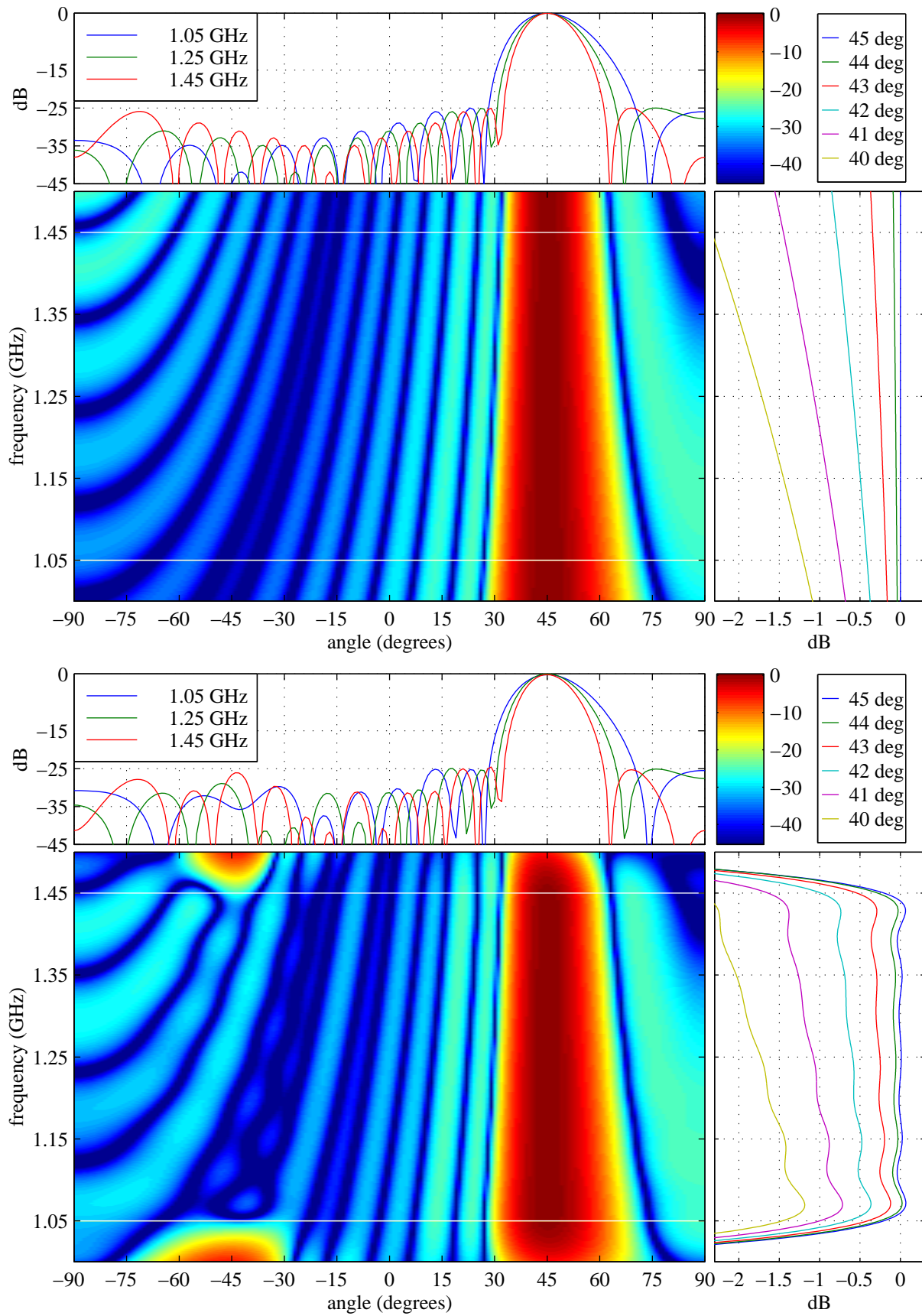


Fig. 1. Ideal time-delay (top) and optimized FIR time-delay (bottom) steered array patterns. The upper-left corner of each response grid show cuts across angle, and the lower-right corner show cuts across frequency.

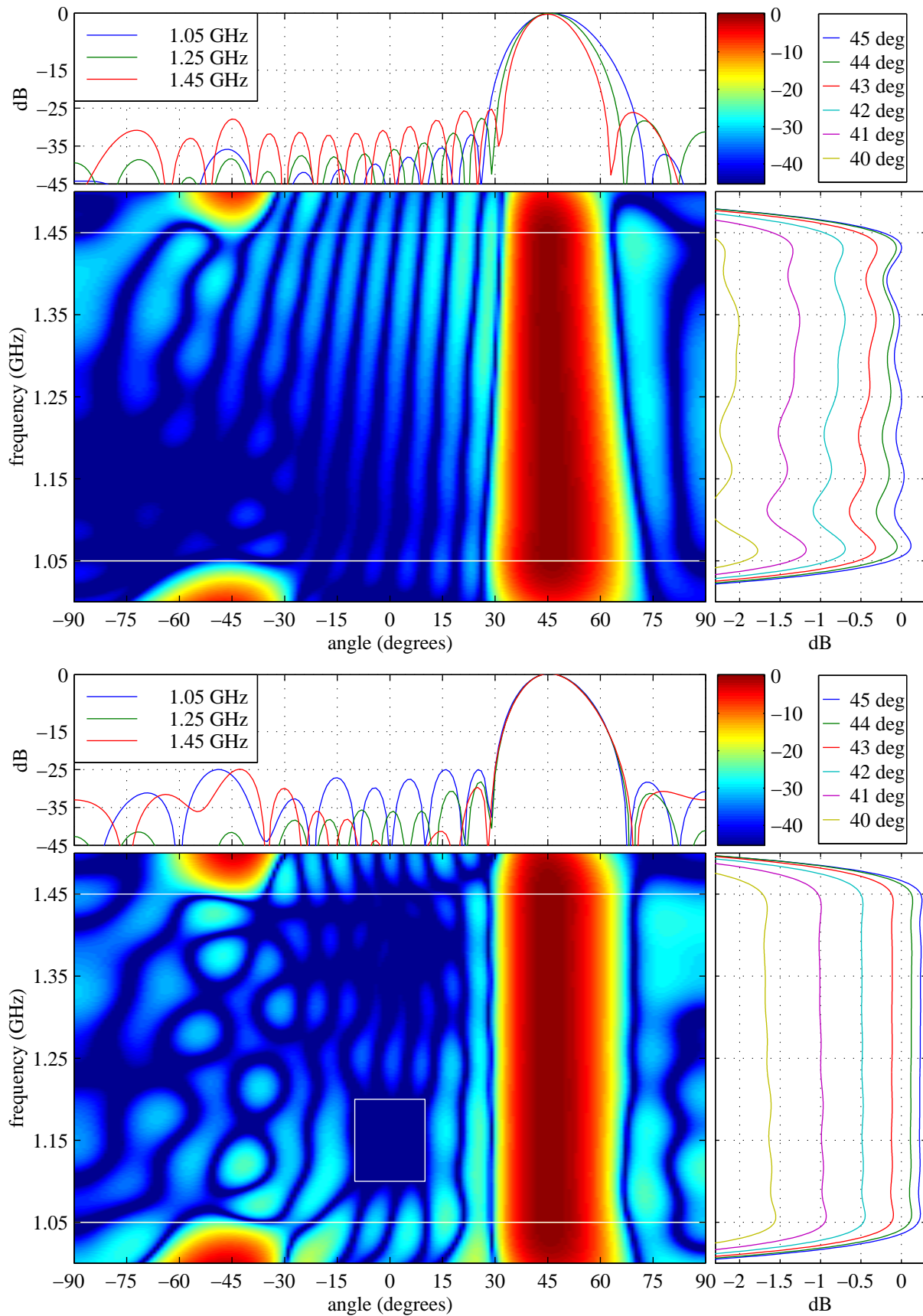


Fig. 2. Optimized wideband array patterns: time-delay-like narrowing main beam (top) and constant-beamwidth (bottom). The small white rectangle in the bottom plot outlines the additional sidelobe constraint region.